On the Measurement of Elastic Constants in Nematic Liquid Crystals: Comparison of Different Methods

Paul R. Gerber and Martin Schadt
F. Hoffmann-La Roche & Co., LTD., Central Research Units, Basel, Switzerland

Z. Naturforsch. **35a**, 1036–1044 (1980); received June 19, 1980

Different methods of measuring elastic constants of nematic liquid crystals by deformation of homogeneously and homeotropically oriented layers through external magnetic and electric fields, respectively, are critically examined. Possible sources of uncertainties are quantitatively explored. An approximative numerical fitting procedure is proposed allowing to take conductivity effects in electrically deformed layers up to large conductivities and/or temperatures into account. A novel, accurate and simple monitoring method to determine twist elastic constants is described. The measurements of the temperature dependence of the splay bend and twist elastic constants of the positive dielectric mixture RO-TN-403 are presented.

1. Introduction

The measurement of elastic constants in nematic liquid crystals is still a rather delicate and complicated matter. This is reflected by the many controversial results published during the past ten years. The most straightforward method to determine elastic constants is via the observation of threshold voltages V_c or threshold magnetic fields H_c in different types of Fréedericksz transitions [1]. For each of the elastic constants k_{11} (splay), k_{22} (twist) and k_{33} (bend) a suitable geometry can be chosen such that the expressions for the threshold voltage, or -field, contain only a single elastic constant given by

$$k_{ii} = \pi^{-2} E_i^{\,a}, \tag{1.1}$$

where $E_i^{\,a}$ is an anisotropy force of the deflecting field taking on the values

$$E_i^{\,a} = \begin{cases} \Delta\chi\, \mu_0 (H_{ic}\, d)^2, & \text{magnetic deflection}, \\ \Delta\varepsilon\, \varepsilon_0 V_{ic}^2, & \text{electric deflection}, \end{cases} \tag{1.2}$$

d = sample thickness, while $\Delta\varepsilon = (\varepsilon_{\parallel} - \varepsilon_{\perp})$ is the dielectric anisotropy and $\Delta\chi$ the magnetic susceptibility anisotropy.

The determination of k_{11} and k_{22} by threshold measurements requires in either case cells with parallel wall alignment; i. e. zero bias tilt angle between the nematic director and the cell boundaries. Therefore, both constants can be determined in the same cell of which the wall alignment can relatively easily be prepared. Direct threshold measurements to determine k_{33} have to be performed in cells with homeotropic surface alignment. However, homeotropic boundaries are more difficult to prepare than homogeneous ones considering the high precision and uniformity required. Therefore, k_{33} is normally determined in tangentially (parallel) aligned cells using either the initial slope of the field-dependent deformation-sensitive quantity used (approximation for small angles of deformation) or the dependence of this quantity over the whole range of field-induced deformation (numerical fitting required). The quantity used to monitor the status of the deformation of the nematic layer is usually either the optical path difference δ between ordinary and extraordinary light ray or the capacitance C of the layer [2, 3]. In one case also the conductivity was used to monitor the deflection [4]. The evaluation of k_{33} from the field-induced dependence of the deformation up to large fields requires numerical fitting of the measurements to the theoretical expressions which are given in a parametric integral representation [3, 5]. The evaluation of k_{33} by analytical expressions derived for small angles of deformation may lead in some cases to rather large errors [6, 7].

The direct determination of k_{22} from threshold measurements is quite elaborate because conventionally the monitoring of the deformation is done by conoscopic observation of the sample between the pole caps of a magnet [8]. Alternatively measurements of the threshold voltage of twisted nematic displays have been used [9–11].

In the past little or no effort has been made to measure elastic constants using different cell

Reprint requests to Dr. P. R. Gerber, F. Hoffmann-La Roche & Co. Ltd., Central Research Units, CH-4002 Basel/Schweiz.

0340-4811 / 80 / 1000-1036 $ 01.00/0. — Please order a reprint rather than making your own copy.

geometries, deflection and detection methods and/or different means of evaluating the experimental findings in order to compare the accuracy and to obtain information on the limits of the respective methods. We believe this to be a major reason for some of the quite large discrepancies between the results published by different workers. Since the elastic constants belong to the most crucial material parameters we have decided to investigate these questions in the following in order to trace down and clarify some of the possible sources of uncertainties.

2. Measurement of k_{11} and k_{33}

The measurement of k_{11} is the least critical one since accurate parallel alignment of the director at the cell surface is obtained by well explored standard techniques [12]. Besides, there are easily accessible ways of monitoring the deflection of the nematic director as well as the threshold fields. The situation becomes more difficult when attempting to determine k_{33} too from measurements made in parallel aligned cells. This approach requires fitting of the optical path difference δ or the cell capacitance C to the respective formulae [3]:

$$[\delta(0)-\delta(f_r)]/\delta(0) = \frac{n_e}{n_0-n_e} \cdot \left[1 - \frac{\int_0^{\varphi_m} d\varphi\,(F_\varkappa F_{\bar\gamma}/F_{-\sigma}F_\nu)^{1/2}}{\int_0^{\varphi_m} d\varphi\,(F_\varkappa F_{\bar\gamma}/F_{-\sigma})^{1/2}}\right], \tag{2.1}$$

$$[C(f_r)-C(0)]/[C(\infty)-C(0)] = \gamma^{-1} \cdot \left[\frac{\int_0^{\varphi_m} d\varphi\,(F_\varkappa F_{\bar\gamma}/F_{-\sigma})^{1/2}}{\int_0^{\varphi_m} d\varphi\,F_\gamma^{-1}(F_\varkappa F_{\bar\gamma}/F_{-\sigma})^{1/2}} - 1\right], \tag{2.2}$$

where f_r designates voltage or field in units of the critical values,

$$\varkappa = \frac{k_{33}}{k_{11}} - 1,$$

$$\nu = \left(\frac{n_e}{n_0}\right)^2 - 1, \quad n_e, n_0 = \text{indices of refraction},$$

$$\gamma = \varepsilon_{\parallel}/\varepsilon_{\perp} - 1, \tag{2.3}$$

$$\bar\gamma = \begin{cases} 0 & \text{for magnetic deflection,} \\ \gamma & \text{for electric deflection,} \end{cases}$$

$$\sigma = \sin^{-2}\varphi_m,$$

with

$$F_\mu(\varphi) = 1 + \mu \sin^2\varphi. \tag{2.4}$$

The integrals are taken to the maximum deflection angle φ_m in the middle of the cell. The connection of φ_m with the field value f_r is given by

$$f_r = \frac{2}{\pi}(\sin^{-2}\varphi_m - \bar\gamma)^{1/2} \int_0^{\varphi_m} \left(\frac{F_\varkappa}{F_{\bar\gamma}F_{-\sigma}}\right)^{1/2} d\varphi. \tag{2.5}$$

From these formulae curves like the ones in Fig. 1 are calculated. They illustrate that the parameter $\varkappa$ has in some cases a fairly limited influence on the shape of the curve which may therefore lead to appreciable uncertainties in the values for k_{33} obtained from a fit to these curves.

An additional source of uncertainty arises from imperfect surface alignment of the director, in particular from out of plane misalignment. In order to get a feeling for the influence of this effect we have measured optical path differences in an applied magnetic field which was aligned not exactly normal to the cell surface but slightly tilted towards the direction of surface alignment. For different tilt angles the measured field dependence of the optical path

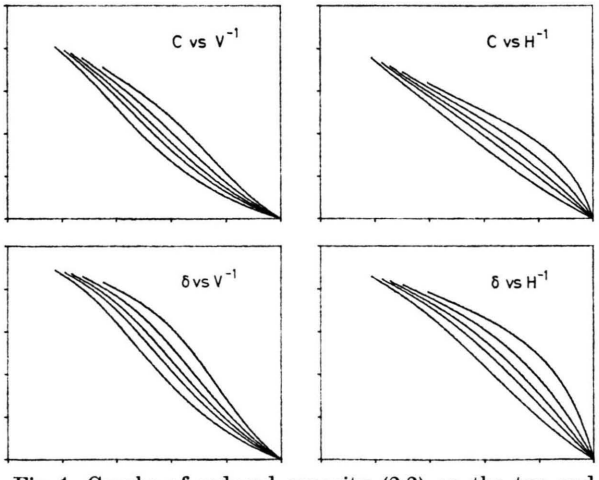

Fig. 1. Graphs of reduced capacity (2.2) on the top and reduced optical path difference (2.1) at the bottom versus reciprocal reduced fields f_r^{-1} (2.5) for electric (left) and magnetic (right) deflection respectively. The scales vary from zero to one when going upwards or to the right. The parameter $\varkappa$ increases from −0.5 (top curves), 0, 0.5, 1.0 to 2.0 (bottom curve). The changes in shape with $\varkappa$ are not particulary significant, $\gamma = 2.0$, $\nu = 0.37$.

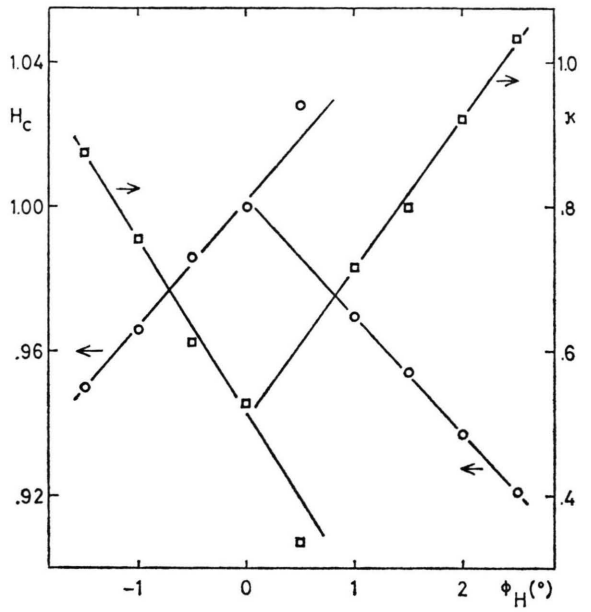

Fig. 2. Values obtained for the critical field H_c (circles, arbitrary units) and the parameter $\varkappa$ (squares) as they result from a fit for which perfect alignment is assumed are shown as functions of the misalignment angle ϕ_H of the magnetic field (misalignment from the normal to the cell surface). By changing ϕ_H in a large field the measurement in the metastable domain at $\phi_H = 0.5°$ was obtained. The temperature was 22 °C.

difference was fitted to a set of material constants pretending in the fit that the field direction was perfectly normal. Fig. 2 shows a plot of these fitted threshold fields and $\varkappa$ values. All measurements have been made with the commercial nematic mixture RO-TN-403 from F. Hoffmann-La Roche [11].

Figure 2 shows that the threshold fields are always lowered for misalignment angles of either sign. The reason for this is that in the case where the magnetic field is not orthogonal to the undeflected nematic director, a stable and a metastable state of deformation exist for high enough fields. The former which is reached usually simulates a lower threshold field. Figure 2 also shows one measurement made on a metastable state. The dependence of the effective threshold field on the misalignment angle has a value of about 3.3% per degree of misalignment which – through the square law dependence of (1.1) – yields for the apparent k_{11}-value changes of 6.6% per degree of misalignment.

Furthermore from Fig. 2 one derives that the fitted value for $\varkappa$ increases by about 0.255 per degree misalignment leading to apparent values of k_{33} which are too large by 7% per degree misalignment. Since these deviations are always of the same sign, imperfect wall alignment leads to the above determined systematic errors for k_{11} and k_{33}. This quantitative finding agrees with the qualitative statements that threshold measurements performed in cells with nonperfect wall alignment tend to give too low values [9, 10].

Another aspect which deserves closer investigation is the importance of separately measured parameters which are not fitted but which are used in the fitting procedure such as the optical anisotropy parameter ν, the dielectric anisotropy parameter γ (2.3) or the cell thickness d which enters through the maximal optical path difference $\delta_{\max}$ or through the maximal capacity change $\Delta C_{\max}$. We have examined the dependence of the fitting procedure on the values of these parameters. The results can be summarized as follows: The values for the threshold voltages or fields are little influenced by changes of these parameters except for the dependence on $\delta_{\max}$, where values of $\partial \ln(V_c)/\partial \ln(\delta_{\max}) \approx -1$ have been found. However, more significant is the dependence of $\varkappa$ on these parameters. While changes in ν or γ are approximately compensated by consequent changes of $\varkappa$ of similar magnitude, the dependence on $\delta_{\max}$ and $\Delta C_{\max}$ are of the order of $\partial \varkappa/\partial \ln(\delta_{\max}, \Delta C_{\max}) \approx 4$. This finding reflects the relatively small influence of $\varkappa$ on the deflection curves as encountered in Figure 1.

Another important question is whether electric or rather magnetic fields should be used for the deflection of the nematic director. The deflection by electric fields is usually more straightforward than the deflection by magnetic fields where even the accurate measurement of the field at the location of the sample may be a tricky procedure due to field-inhomogeneities, temperature dependence of the Hall-probe and so on. However, the advantages of electric-field-induced alignment may be diminished by effects due to the conductivity of liquid crystal materials. The conductivity increases exponentially with temperature and depends very critically on even slight ionic impurities that may contaminate the cell surfaces. Therefore, conductivity effects often play an important role and have to be taken into account in the measurements as well as in the evaluation of the results. Gruler and Cheung [13] have calculated the effects of conductivity on the deformation of nematic layers by electric fields for

small angles of deformation. In Appendix I we extend these calculations and derive the corresponding formulae for larger deformations. However, since the conductivities may vary from cell to cell and perhaps even from spot to spot within a cell their determination is very difficult. But with ambiguous conductivity values the formulae of Appendix I are of little use when attempting to get more accurate values for $\varkappa$ from electric deformation measurements. Therefore we propose in Appendix I a procedure which takes conductivity effects into account in an approximate manner.

The approximation consists in replacing the experimentally determined γ-value in the formulae for the nonconducting case in case where conductivity exists by an effective value γ_{eff} which is adjusted to give an optimal fit to the measured field-dependent deformation of the nematic layer. Although a somewhat heuristic approach, this procedure has yielded values for V_c and $\varkappa$ which are essentially independent of conductivity. This is shown in Fig. 3 where the fitted values are displayed as a function of the loss angle $\operatorname{tg}\beta = G_\perp/(\omega C_\perp)$; $G_\perp$ = perpendicular sample conductance. Fitting with the γ-value obtained from static dielectric measurements yields only good results for small β-values, whereas the adjustable-γ_{eff} approach yields satisfactory results even for $\operatorname{tg}\beta \approx 1$. From these findings follows that the proposed procedure makes the deflection by electric fields a usefull and simple method to determine k_{11} and k_{33} even at elevated temperatures where strong conductivity increases occur.

At this point we would like to make a comparison between the results obtained by the different procedures, namely a comparison between results obtained from deflection by electric and magnetic fields respectively as well as a comparison between the capacitive and optical detection of the nematic deformation. Table 1 shows the data for the threshold- and $\varkappa$-values for RO-TN-403 at room temperature. An important comparison is the one between optical and capacitive monitoring. The latter shows systematically lower threshold- and higher $\varkappa$-values. With the previous findings on the angular dependence of these quantities we are inclined to attribute this difference to the fact that for the optical measurement a uniform spot can be selected within the cell while in the capacitive case an average is taken over a large area which always contains imperfections and slightly tilted regions. Table 1 also shows

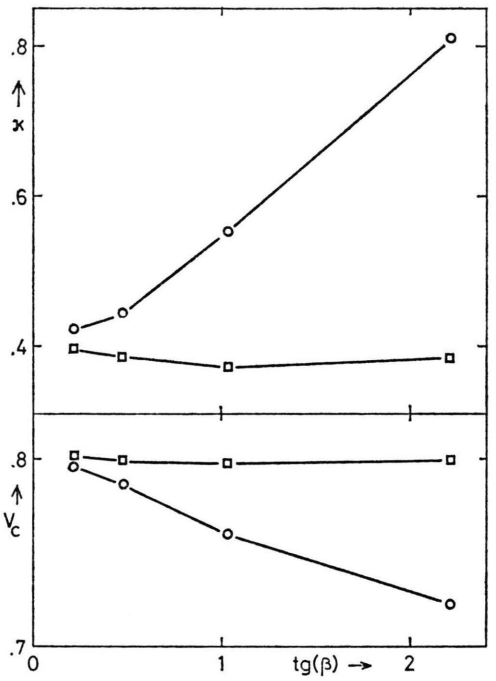

Fig. 3. Values for V_c in volts and $\varkappa$ as obtained from a fitting procedure with the experimentally determined value of γ (circles) and with an adjustable γ_{eff} (squares) as a function of $\operatorname{tg}\beta = \sigma_\perp/(\varepsilon_\perp \varepsilon_0 \omega)$. The procedure using the adjustable γ_{eff} leads to almost constant values of V_c and $\varkappa$ (despite $\beta > 0$) which are equal to the limiting values ($\beta = 0$) which one obtains when using the fixed-γ fitting procedure! β was changed by changing the frequency of the driving voltage. For this substance $\Delta\sigma/\sigma_\perp$ was 0.67 and $\gamma = 2.95$. The temperature was 43 °C.

that optimizing the fit by adjusting γ causes $\varkappa$ as determined from electric-field deformation measurements to approach the value obtained from magnetic-field deflection experiments; i. e. better agreement between the two deflection methods is obtained than in the case where fixed γ-values are used.

Table 1. Critical voltage V_c in volts and Gauss · cm and corresponding $\varkappa$ values as obtained for electric (e) and magnetic (m) deflection respectively, using capacitive (C) or optical (O) monitoring for TN-403 at 22 °C. In the electrical case two fitting procedures with γ fixed (f) and γ adjustable (a) have been applied. The threshold for a cell with homeotropic wall alignment (h) and the corresponding $\varkappa$ value is shown in the last column.

Method	mC	mO	eCf	eOf	eCa	eOa	h
V_c	8.52	8.59	.835	.846	.832	.839	10.66
$\varkappa$	.593	.555	.707	.611	.612	.536	.535

The results of Table 1 indicate that the determination of thresholds involves uncertainties of $\lesssim \pm 2\%$ leading to error limits of $\lesssim \pm 4\%$ for k_{11}. The uncertainty in the determination of $\varkappa$ is found to be $\lesssim 0.05$. These limits have been confirmed in a series of similar measurements which will be published in a different context. We tend to consider the preparation of the cell surfaces to be the limiting factor determining the accuracy of k_{ii} measurements. Uniform wall alignment over large electrode areas with bias tilt angles $\lesssim 0.5°$ are difficult to achieve. Considering this small residual bias tilt and the above findings we believe it to be very difficult to determine $\varkappa$ with any of the above methods such that (i) the resulting accuracy is substantially better than indicated in Table 1 and (ii) that the result is compatible with all of the above mentioned methods which we consider to be comparably suitable to determine k_{ii}.

To compare the results obtained for k_{33} from measurements made with parallel aligned cells with an additional method we performed some experiments with homeotropically aligned cells allowing to measure k_{33} directly from a threshold field. Homeotropic boundaries were obtained by treating the cell surfaces with a solution of a 0.4% lecithine in ethanol. Table 1 shows the room temperature value of the (homeotropic) threshold field measured in a 20 μm cell. The same column (Table 1) shows the value of $\varkappa$ determined from the homeotropic threshold field as well as from the value of k_{11} measured in a parallel aligned cell. This value of $\varkappa$ is in fair agreement with the ones measured in parallel aligned cells (Table 1). Regarding the difficulties to obtain perfectly aligning and temperature resistant homeotropic boundaries and considering the necessity that two differently aligned cells have to be used to determine all three elastic constants, we prefer – as most authors do – to use a single homogeneously aligned cell to measure k_{11} and k_{33} simultaneously.

3. Measurement of k_{22}

The determination of k_{22} is often made through measurements of the threshold voltage of twist cells [9–11].

$$V_{\mathrm{c,twist}} = V_{\mathrm{c,hom}} \sqrt{1 + \frac{1}{4}(1+\varkappa) - \frac{1}{2}\frac{k_{22}}{k_{11}}}\,. \qquad (3.1)$$

This procedure is very delicate because k_{22} does not enter very significantly in (3.1). Besides three quantities with independent uncertainties are involved in (3.1). As an illustration we take our measurements for RO-TN-403 which are $V_{\mathrm{c,twist}} = 0.869\,\mathrm{V} \pm 2\%$, $V_{\mathrm{c,hom}} = 0.839\,\mathrm{V} \pm 2\%$, $\varkappa = 0.55 \pm 0.05$. Inserting these data in (3.1) yields

$$k_{22}/k_{11} = 0.63 \pm 0.12\,. \qquad (3.2)$$

The resulting very large uncertainty of $\pm 20\%$ exemplifies the ambiguity of this method. With the small variations in k_{22}/k_{11} generally encountered among different nematics it is obvious that the more reliable method of inducing a pure twist configuration in a homogeneous cell by a magnetic field [8] should be used to determine k_{22}. The handicap of this method so far was that conventionally visual observation of a conoscopic pattern was used to monitor the deflection of the director [8]. The necessity of conoscopic observation was deduced from the assumption of adiabatic light propagation through the twisted structure [1, 8]. In Appendix II we show that by going to the next higher approximation one can expect to monitor also a signal for parallel light travelling normal to the cell surfaces. Our experiments prove this signal to be sufficiently intense to allow reliable monitoring of the field-induced twist deformation of homogeneous nematic layers. In the experimental arrangement polarizer and analyser are crossed and aligned parallel or perpendicular to the nematic director at the surfaces. Careful adjustment of these directions is achieved by minimizing the transmitted light intensity in the undeflected state. When raising the field above the threshold voltage one observes an increase of light intensity. This increase is maximized by adjusting the wavelength of the light such that the optical phase difference between ordinary and extraordinary ray becomes approximately an odd multiple of one half (see Appendix II). Now the signal shows an asymptotically linear dependence on the excess magnetic field thus allowing to determine the threshold field in a straightforward way. Figure 4 shows a measurement of the transmitted light intensity versus applied magnetic field. The adjustment of the wavelength proved to be important for obtaining graphs with a sharp threshold. In unfavourable cases mistuning resulted in rounded curves, as one might expect from higher order effects. The determination of the threshold field using this method is possible within a few percent. For RO-TN-403 we obtain

$$k_{22}/k_{11} = 0.53 \pm 0.03\,, \qquad (3.3)$$

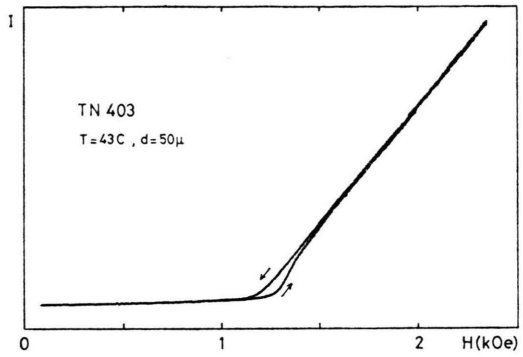

Fig. 4. Transmitted light intensity versus applied magnetic field as observed in the arrangement to determine the threshold field for twist deformations in parallel aligned cells. This detection method using parallel collimated light propagating perpendicular to the cell walls allows the accurate determination of the threshold. The sweeping speed was 0.9 Oe/sec.

a value which is perfectly consistent with the threshold voltage measured in a twisted nematic cell. The method to determine k_{22} requires the knowledge of $\Delta\chi$ which we can extract from the measured threshold-voltages and -magnetic fields tabulated in Table 1 using (1.1) and (1.2).

Regarding the accuracy of this method to determine k_{22} the most important factor again appears to be the quality of the surface alignment which has a comparable influence on the threshold field as found for the measurements of k_{11}. Hence one can except the values of k_{22} to become systematically too low if the direction of the magnetic field deviates from the normal with respect to the nematic director at the cell walls. A $\pm 4\%$ uncertainty is thus given for k_{22} too.

Finally we show in Fig. 5 the temperature dependence of the measured elastic constants of RO-TN-403. Magnetic and electric (with adjusting γ) deflection have been used together with optical monitoring to obtain k_{11} and $\varkappa$. Also show is

$$\varkappa_2 = k_{22}/k_{11} - 1 \tag{3.4}$$

as obtained from measurements of pure twist deformation threshold (Figure 4). From these values one can calculate a quantity

$$\bar{\varkappa} = \frac{1}{4}\varkappa - \frac{1}{2}\varkappa_2 - \frac{1}{4} \tag{3.5}$$

which is also plotted in Figure 4. Besides the quantity $\varkappa_t$ is shown which is given by

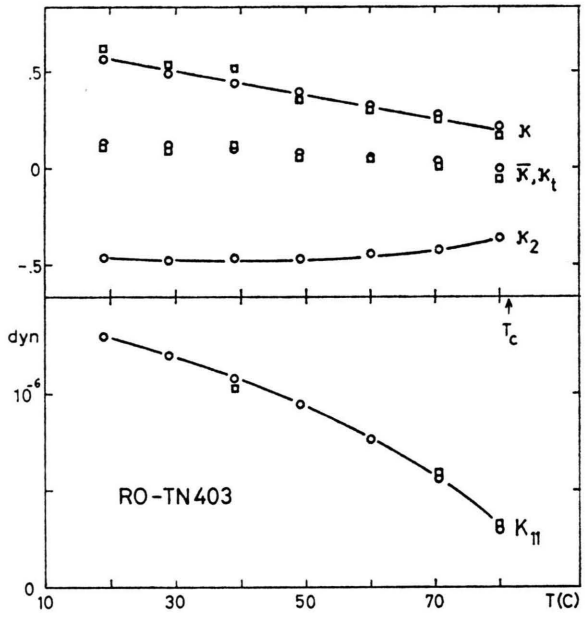

Fig. 5. Measured temperature dependence of the elastic constants of RO-TN-403. For k_{11} and $\varkappa$ the circles show measurements made by magnetic deflection, whereas squares show measurements made by electric deflection using the adjustment procedure with γ_{eff}. In the measurement of k_{11} the squares were omitted where they coincided with the circles. The twist constants ($\varkappa_2$) are obtained from threshold measurements made in parallel aligned cells in which field-induced twist was generated. The results yield $\bar{\varkappa}$ values (Eq. (3.5) squares) which are cross-checked by comparisons with threshold measurements made in twisted nematic displays represented as $\varkappa_t$ (Eq. (3.6) shown as circles). $\Delta\chi$ was taken to be proportional to Δn.

$$\varkappa_t = \left(\frac{V_{c,\text{twist}}}{V_{c,\text{hom}}}\right)^2 - 1 . \tag{3.6}$$

Both quantities $\bar{\varkappa}$ and $\varkappa_t$ should be identical within experimental uncertainties. Figure 5 shows indeed quite satisfactory agreement between $\varkappa_t$ and $\bar{\varkappa}$ up to temperatures approaching T_c, thus indicating again that the measurements and the evaluation of k_{11}, k_{22} and k_{33} presented here are consistent.

Earlier measurements [11] gave $k_{11} = 12.6 \cdot 10^{-12}$ N, $k_{22} = 10.8 \cdot 10^{-12}$ N and $k_{33} = 23.11 \cdot 10^{-12}$ N at room temperature. These data have to be compared with the present values $k_{11} = 12.6 \cdot 10^{-12}$ N, $k_{22} = 9.3 \cdot 10^{-12}$ N and $k_{33} = 17.6 \cdot 10^{-12}$ N. We have tried to extract a value for k_{33} from an initial slope evaluation of the measured $C(V)$ dependence. The main difficulty when using this approach is that the curve exhibits a fairly long straight initial portion starting closely above threshold from which one is

tempted to extract the initial slope. However, this evaluation yielded values of $k_{33} \approx 13.4 \cdot 10^{-12}$ N. Besides this straight portion a sort of a slight modulation of the $C(V)$-dependence just above threshold was measured. By making a plausible extrapolation from this part of the graph one obtains values for k_{33} up to $20 \cdot 10^{-12}$ N. As it is very difficult to distinguish the small $C(V)$-fluctuations from spurious threshold effects like rounding-off due to misalignment or inadequate sweeping speeds, we tend to attribute the descrepancies with the earlier measurements of k_{33} to this problem. Other reasons for the discrepancy may be inaccuracies in the determination of the conductivities and/or more likely errors following from uncertainties in the determination of k_{22} from twist cell threshold voltages as discussed at the beginning of this section.

4. Summary

We have made a quantitative examination of some important sources of ambiguity and error that are often neglected in measurements and their evaluation of elastic constants of nematic liquid crystals. Crucial sources of errors were found to be the misalignment of electric or magnetic deflecting fields and/or misalignment of the nematic director at the cell boundaries. We have shown the influence of small angle approximations on the accurracy in the determination of the bend elastic constant k_{33} and examined the influence of conductivity effects on the measurements when using electric fields to deform nematic layers. It is shown that capacitive monitoring of field-induced deflection may lead to systematic errors in the determination of elastic constants due to the always present imperfections in large measuring areas of sample cells. We have devised a numerical fitting procedure which allows to use electric field-induced deflection of the nematic director to determine k_{ii} in actual, i. e. nonperfectly isolating liquid crystal samples. The results obtained when measuring k_{ii} up to temperatures approaching the nematic-isotropic transition of mixture RO-TN-403 are comparable to those found for magnetic field deflection. Measurements of twist elastic constants via the determination of threshold voltages of twisted nematic cells are shown to be very delicate. We propose a simple method for monitoring field-induced distortions in twisted nematic configurations leading to an accurate determination of k_{22}. The experiments were performed over a wide temperature range using magnetic and electric field deflection in homogeneously and homeotropically aligned nematic samples respectively, as well as using capacitive and optical detection methods.

Appendix I. Conductivity Induced Alignment

Following Gruler and Cheung [13] we start from the torque balance equation

$$\frac{\varepsilon_0 \Delta\varepsilon}{k_{11}} E^2 \sin\varphi \cos\varphi + (1 + \varkappa \sin^2\varphi) \frac{\mathrm{d}^2\varphi}{\mathrm{d}z^2} + \varkappa \sin\varphi \cos\varphi \left(\frac{\mathrm{d}\varphi}{\mathrm{d}z}\right)^2 = 0 \qquad \text{(A 1.1)}$$

where the angle φ by which the director is deflected from its equilibrium position in the field-free case depends on the coordinate z normal to the cell surfaces. Instead of the dielectric displacement D which is independent of z in the non conducting case we have in the conducting case the condition [13]

$$J \equiv \sigma E + \dot{D} = \text{const}, \qquad \text{(A 1.2)}$$

where σ is the conductivity tensor. For a pure alternating current and neglecting space change effects we replace E^2 in (A 1.1) by the RMS-value

$$\frac{1}{2} E E^* = \frac{J J^*}{2 \varepsilon_0^2 \omega^2} \left[\varepsilon^2 + \left(\frac{\sigma}{\omega \varepsilon_0}\right)^2\right]^{-1}, \qquad \text{(A 1.3)}$$

where ε and σ denote the values of the dielectric constant and the conductivity in the direction normal to the cell plane therefore depending on the orientation of the director. This procedure assumes that the frequency ω is high enough to prevent the director from following the ac-motion. With the expressions

$$\begin{aligned} \varepsilon &= \varepsilon_\perp + \Delta\varepsilon \sin^2\varphi, \\ \sigma &= \sigma_\perp + \Delta\sigma \sin^2\varphi, \end{aligned} \qquad \text{(A 1.4)}$$

the torque balance equation takes the form

$$\frac{d}{\mathrm{d}z}\left[(1 + \varkappa \sin^2\varphi)\left(\frac{\mathrm{d}\varphi}{\mathrm{d}z}\right)^2 - C A(\varphi)\right] = 0, \qquad \text{(A 1.5)}$$

where

$$C = \frac{J J^*}{\varepsilon_0 \varepsilon_\perp \omega^2 k_{11}}, \qquad \text{(A 1.6)}$$

and

$$\mathrm{A}(\varphi) = \alpha^{-1} \operatorname{arcot}\left\{\left[1 + \frac{\sigma_\perp \Delta\sigma}{\varepsilon_\perp \Delta\varepsilon\, \varepsilon_0 \omega^2} + \sin^2\varphi \left(\Delta\varepsilon^2 + \frac{\Delta\sigma^2}{\varepsilon_0^2 \omega^2}\right) \Big/ (\varepsilon_\perp \Delta\varepsilon)\right] \Big/ \alpha\right\}, \qquad \text{(A 1.7)}$$

with

$$\alpha = \frac{\Delta\sigma}{\Delta\varepsilon\, \varepsilon_0 \omega} - \frac{\sigma_\perp}{\varepsilon_\perp \varepsilon_0 \omega}. \qquad \text{(A 1.8)}$$

For vanishing conductivity this reduces to

$$A(\varphi) \approx (1+\gamma \sin^2\varphi)^{-1}, \quad \sigma, \ \Delta\sigma \to 0, \quad \text{(A 1.9)}$$

yielding the known cases [3, 5]. The detection of the optical path difference is determined by an average etraordinary refractive index given by [2]

$$\langle n \rangle = \frac{1}{d}\int_0^d n(\varphi(z))\,\mathrm{d}z\,. \quad \text{(A 1.10)}$$

In our case this integral takes the form

$$\langle n \rangle = n_e \int_0^{\varphi_m} \mathrm{d}\varphi \left\{\frac{1+\varkappa \sin^2\varphi}{(1+\nu\sin^2\varphi)\,[A(\varphi)-A(\varphi_m)]}\right\}^{1/2} \Bigg/ \int_0^{\varphi_m} \mathrm{d}\varphi \left\{\frac{1+\varkappa\sin^2\varphi}{A(\varphi)-A(\varphi_m)}\right\}^{1/2}. \quad \text{(A 1.11)}$$

For the voltage accross the cell one obtains

$$\frac{V_{\mathrm{eff}}}{V_c} = \frac{2}{\pi}\sqrt{\gamma}\int_0^{\varphi_m} \frac{\mathrm{d}\varphi}{\left|1+i\dfrac{\sigma_\perp}{\varepsilon_\perp \varepsilon_0 \omega}+\sin^2\varphi\left(\gamma+i\dfrac{\Delta\sigma}{\varepsilon_\perp\varepsilon_0\omega}\right)\right|} \cdot \left\{\frac{1+\varkappa\sin^2\varphi}{A(\varphi)-A(\varphi_m)}\right\}^{1/2}. \quad \text{(A 1.12)}$$

It follows from (A 1.7), (A 1.8) and (A 1.12) that the conductivity has no effect on the functional forms when $\Delta\sigma/\sigma = \gamma$. However, in reality this situation is unlikely to occur. With unknown values for σ and $\Delta\sigma$ one may try to replace the integrals in (A 1.11) and (A 1.12) by the ones for the nonconducting limiting case ($\sigma = \Delta\sigma = 0$) but leaving γ as an adjustable parameter. This procedure is certainly a fair approximation for small conductivities (e. g. $\sigma_\perp/(\varepsilon_\perp\varepsilon_0\omega) \ll 1$). It proves to be correct in a linearized form for small excess field where an effective value

$$\gamma_{\mathrm{eff}} = \gamma\left[1+\frac{\sigma_\perp \Delta\sigma}{\varepsilon_\perp \Delta\varepsilon(\omega\varepsilon_0)^2}\right]\Bigg/\left[1+\left(\frac{\sigma_\perp}{\varepsilon_\perp\omega\varepsilon_0}\right)^2\right] \quad \text{(A 1.13)}$$

replaces γ in the formulae for the nonconducting case [13]. For high conductivities ($\sigma/(\varepsilon\varepsilon_0\omega) \gg 1$) the procedure becomes exact again with γ replaced by $\gamma_{\mathrm{eff}} = \Delta\sigma/\sigma_\perp$ as can be seen from (A 1.7) and (A 1.12). For intermediate cases this heuristic procedure still proves to be usefull, cf. Section 2.

Appendix II. Monitoring Twist Deformations in Planar Configurations

We consider a nematic layer aligned parallel to the $\bar{x}$-$\bar{y}$-plane; the director has the components $n = [\cos\varphi(z), \sin\varphi(z)]$ lying always in the $\bar{x}$-$\bar{y}$-plane. At the boundaries ($z = \pm d/2$) it points in the $\bar{x}$-direction, $\varphi(\pm d/2) = 0$. We introduce a local coordinate system (x, y) bound to the nematic director which is rotated by an angle φ with respect to the fixed system $(\bar{x}, \bar{y})$. In the rotated system n points always in the x-direction. In this coordinate system the equations of propagation of planar electromagnetic waves along the z-direction read for the electric field E

$$\begin{aligned} E_x'' &= +\varphi'' E_y + 2\varphi' E_y' - [p_0^2 n_e^2 - (\varphi')^2]E_x\,, \\ E_y'' &= -\varphi'' E_x - 2\varphi' E_x' - [p_0^2 n_0^2 - (\varphi')^2]E_y\,, \end{aligned} \quad \text{(A 2.1)}$$

where primes denote derivatives with respect to z, and $p_0 = \omega/c$. We assume only long wavelength distortions of the nematic to occur i. e.

$$\varphi' \ll p_0(n_e - n_0), \ \varphi'' \ll \varphi' p_0\,. \quad \text{(A 2.2)}$$

The zeroth approximation for the solution of (A 2.1) gives the adiabatically guided light

$$\underset{y}{E_x} = \underset{y}{E_{x,0}} \exp\{\pm i p_0 \underset{0}{n_e} z\}\,. \quad \text{(A 2.3)}$$

For the next approximation we assume slowly z-dependent amplitudes $E_{x,0}(z)$ and $E_{y,0}(z)$. We further restrict ourselves to the experimental conditions $E_{y,0}(z = -d/2) = 0$. Since we restrict ourselves to a limited total twist $|\varphi| < \pi/2$ in the first approximation we can assume $E_{x,0} = \text{constant}$. This yields

$$E_{y,0}' \approx E_{x,0}\frac{n_e}{n_0}\varphi' \exp\{i p_0(n_e - n_0)z\}\,, \quad \text{(A 2.4)}$$

and after integration

$$E_{y,0}\left(\frac{d}{2}\right) = E_{x,0}\frac{n_e}{n_0}\int_{-d/2}^{d/2}\varphi'(z)\exp\{i p_0(n_e-n_0)z\}\,\mathrm{d}z\,. \quad \text{(A 2.5)}$$

With the functional dependence

$$\varphi'(z) = A\sin\left(\frac{\pi}{d}z\right)$$

as found just above the Fréedericksz transition in the experimental arrangement of Sect. 3 one obtains

$$E_{y,0}\left(\frac{d}{2}\right) = i E_{x,0}\frac{n_e}{n_0} A \frac{4d}{\pi}\frac{w\cos\pi w}{1-4w^2}\,,$$

$$w = \frac{d p_0}{2\pi}(n_e - n_0)\,.$$

Thus, large optical changes occur at the maxima of this function, i. e. near the values $w = 1, 2, \ldots$

where ordinary and extraordinary ray are shifted by an odd multiple of half a wavelength.

For the detection of the Fréedericksz transition of Sect. 3 one must keep in mind that the amplitude A of the deformation varies as $\sqrt{H-H_c}$. This leads to a linear dependence on $(H-H_0)$ of the intensity $(\sim A^2)$ observed for light polarized in y-direction after leaving the cell.

[1] For a general review see for instance P. G. de Gennes, The Physics of Liquid Crystals, Clarendon Press Oxford 1974, and References therein.
[2] A. Saupe, Z. Naturforsch. **15a**, 815 (1960).
[3] H. Gruler. T. J. Scheffer, and G. Meier, Z. Naturforsch. **27a**, 966 (1972).
[4] F. Schneider, Z. Naturforsch. **28a**, 1660 (1973).
[5] H. Deuling, Mol. Cryst. Liq. Cryst. **19**, 123 (1972).
[6] H. Schad, B. Scheuble, and J. Nehring, J. Chem. Phys. **71**, 5140 (1979).
[7] R. J. A. Tough and E. P. Raynes, Mol. Cryst. Liq. Cryst. **56L**, 19 (1979).
[8] P. E. Cladis, Phys. Rev. Lett. **28**, 1629 (1972).
[9] W. H. de Jeu, W. A. P. Classen, and A. M. J. Spruijt, Mol. Cryst. Liq. Cryst. **37**, 269 (1976).
[10] W. H. de Jeu and W. A. P. Classen, J. Chem. Phys. **67**, 3705 (1977).
[11] M. Schadt and F. Müller, IEEE Transactions **Ed15**, 1125 (1978).
[12] E. Guyon, P. Pieranski, and M. Boix, Lett. Appl. Eng. Sci. **1**, 19 (1973).
[13] H. Gruler and L. Cheung, J. Appl. Phys. **46**, 5097 (1975).